

# Electronic Structure of Samarium Monopnictides and Monochalcogenides

A. Svane<sup>1</sup>, V. Kanchana<sup>2</sup>, G. Vaitheeswaran<sup>2</sup>, G. Santi<sup>1</sup>,  
W. M. Temmerman<sup>3</sup>, Z. Szotek<sup>3</sup>, P. Strange<sup>4</sup> and L. Petit<sup>1,5</sup>

<sup>1</sup>*Department of Physics and Astronomy,*

*University of Aarhus, DK-8000 Aarhus C, Denmark*

<sup>2</sup>*Max-Planck-Institut für Festkörperforschung, D-70569 Stuttgart, Germany*

<sup>3</sup>*Daresbury Laboratory, Daresbury, Warrington WA4 4AD, United Kingdom*

<sup>4</sup>*Department of Physics, Keele University, ST5 5DY, United Kingdom and*

<sup>5</sup>*Computer Science and Mathematics Division, and Center for Computational Sciences, Oak Ridge National Laboratory, Oak Ridge, TN 37831, USA*

(Dated: March 22, 2022)

The electronic structures of SmX (X=N, P, As, Sb, Bi, O, S, Se, Te, Po) compounds are calculated using the self-interaction corrected local-spin density approximation. The Sm ion is described with either five or six localized  $f$ -electrons while the remaining electrons form bands, and the total energies of these scenarios are compared. With five localized  $f$ -electrons a narrow  $f$ -band is formed in the vicinity of the Fermi level leading to an effective intermediate valence. This scenario is the ground state of all the pnictides as well as SmO. With six localized  $f$ -electrons, the chalcogenides are semiconductors, which is the ground state of SmS, SmSe and SmTe. Under compression the Sm chalcogenides undergo first order transitions with destabilization of the  $f$  states into the intermediate valence state, the bonding properties of which are well reproduced by the present theory.

PACS numbers: 71.20.Eh, 71.28.+d, 71.15.Mb, 71.15.Nc

## I. INTRODUCTION

The valency of rare earth compounds continues to be a vivid research area.<sup>1,2,3,4,5,6,7,8,9</sup> Of particular interest are systems where valency is influenced by controllable external parameters like pressure, temperature or alloying. Several systems with varying or fluctuating valencies are known.<sup>1,10</sup> One of the most studied systems is SmS,<sup>1,11,12,13</sup> which at low temperature and zero pressure crystallizes in the NaCl structure with a semiconducting behavior, in accordance with the presence of divalent Sm ions and a full S  $p$ -band. At a moderate pressure of  $\sim 0.65$  GPa SmS reverts to a metallic phase with a significant volume collapse of 13.5%,<sup>14</sup> however retaining the NaCl structure. At very low temperature, the high pressure phase in fact reveals a small pseudogap, of the order of  $\sim 7$  meV.<sup>1</sup> Photoemission experiments show distinctly different spectra for the two phases, which usually are interpreted on the basis of divalent  $f^6$  ions in the ground state and mixed valent  $f^5 - f^6$  ions in the high pressure metallic phase.<sup>15,16</sup> Recent experiments also find indications of small amounts of  $f^5$  character in the ground state.<sup>7</sup> The  $C_{12}$  elastic constant decreases with pressure<sup>17</sup> and becomes negative in the high pressure phase, indicative of an intermediate valence system.<sup>1</sup> The pressure induced semiconductor to metal transformation has also been traced by optical reflectivity studies,<sup>18</sup> Mössbauer measurements,<sup>19</sup> resistivity measurements,<sup>20</sup> and inelastic X-ray scattering.<sup>8</sup> Valence transitions can also be brought about by alloying with other trivalent ions, such as Y, La, Ce or Gd, into the SmS lattice.<sup>1,21</sup> Similar valence instabilities are observed in SmSe and SmTe,<sup>2,11,15,20</sup> which also crystallize in the NaCl structure. For these compounds the volume

changes continuously, but anomalously, with compression (at room temperature).<sup>2,22</sup> From the photoemission studies it is concluded that SmSe and SmTe at ambient pressure, like SmS, are also of predominantly  $f^6$  character,<sup>15</sup> while the monopnictides show clear signals of pure  $f^5$  ions.<sup>15,23</sup>

The present paper addresses two issues of the SmX compounds. Firstly, density functional based total energy calculations are used to investigate the ground state valency of Sm. To validate the approach, calculated values of lattice constants and (for the Sm chalcogenides) valence transition pressures are compared to experiment. Secondly, electron spectral functions are calculated by combining the band structure Hamiltonian of the total energy calculation with an atomic description of the multiplets of the localized  $f$  electrons.

The theoretical description of Sm compounds is a challenge due to the Sm  $f$ -electrons. Conventional band structure calculations of SmS,<sup>3,24,25,26</sup> as implemented within density functional theory<sup>27</sup> in the local density approximation (LDA), describe the  $f$  electrons as narrow bands. A spin-orbit splitting of about 0.6 eV between occupied  $4f_{5/2}$  and unoccupied  $4f_{7/2}$  bands is found, and the valency transition can be traced by the crossing of the occupied  $f$  bands with the lowest  $d$  conduction band upon compression.<sup>25</sup> However, the bonding of the  $f$  electrons when described as band states is greatly overestimated, as the calculated lattice constant of SmS from the LDA calculations is 7.6% smaller than the experimental value.<sup>26</sup> To treat the  $f$  electrons as localized, Schumann et al.<sup>3</sup> applied self-interaction corrections (SIC) to the six  $4f_{5/2}$  states. This led to a semiconducting ground state of SmS, however with a too wide gap of charge transfer type, from S  $p$  to Sm  $d$  bands, in contrast to the Sm

$f$  to  $d$  character inferred from experiment.<sup>1</sup> The reason is that the SIC scheme does not position the energy of the localized  $f$  states properly with respect to the band states. While the formalism does lead to some SIC  $f$  eigen-energies (which formally are just Lagrange multiplier parameters of the theory with no physical interpretation), these are poor representations of the physical removal energies due to the localized nature of the excitations. To remedy this, subsequent work of Lehner et al.<sup>4</sup> calculated the spectral density of SmS using a multi-band periodic Anderson model, in which the  $s$ ,  $p$ , and  $d$  states were treated as band states within LDA, while the  $4f$  states were treated as localized states including atomic multiplets. The calculated spectral density was found to be in good agreement with the measured photoemission and inverse photoemission spectra. Recently, the electronic structure and optical spectra of SmS, SmSe and SmTe were calculated with the LSDA+U approach.<sup>6</sup> This scheme includes an effective Coulomb parameter to separate bands of occupied and unoccupied correlated electrons. Some ambiguity exists as to how this is most appropriately done,<sup>28</sup> but the implementation of Ref. 6 leads to good agreement with experimental optical spectra, although multiplet effects still have to be considered separately.

In the present work the research efforts outlined above will be pursued further. The trends of the electronic structures of all of the samarium pnictides and chalcogenides will be investigated. We separate the issues of total energy and ground state determination from that of excited states properties. The total energy is calculated using the self-interaction corrected local-spin density (LSD) approximation.<sup>29</sup> When applied to rare earth systems this scheme may describe the electron states as either localized or delocalized.<sup>5</sup> For Sm compounds the relevant scenarios would have either 5 or 6 localized  $f$ -electrons on each Sm atom, corresponding to a trivalent or divalent Sm ion, respectively, and by comparison of the total energy the ground state configuration can be determined. The details of the SIC-LSD approach and its implementation will be presented in Section II.A of this paper. The SIC-LSD method is primarily suitable for calculating ground state configurations, crystal structure and equilibrium lattice constants. Results for these parameters are presented in Section III, including the discussion of pressure induced valency transitions. The photoemission spectra of SmX compounds are discussed by comparison to calculated spectral functions. The density of states from a total-energy calculation cannot be directly compared with experimental photoemission spectra. This is particularly clear in systems with partly filled localized shells, where photoemission spectra reflect the multiplet structure of the final state. To include these effects, in the present work the LDA band Hamiltonian is combined with additional atomic multiplet information, which is calculated in an isolated reference atom in the Hubbard-I approximation.<sup>30</sup> The technical details of the present implementation<sup>31</sup> are discussed in Section

II.B. In Section III the calculated spectral functions are presented and discussed in relation to experimental photoemission spectra. Finally, Section IV contains the conclusions of the present work.

## II. THEORY

Two important theoretical tools are employed in this work for the investigation of the electronic structure of SmX compounds. The ground state total energies are calculated with the self-interaction corrected local-spin-density method,<sup>29,32</sup> while the spectral functions are evaluated with the 'LDA++Hubbard I' atomic corrections method.<sup>31</sup>

### A. The SIC-LSD total-energy method

The starting point is the total energy functional of the LSD approximation, which is renowned for its chemical accuracy in describing conventional weakly correlated solids.<sup>33</sup> The essential approximation is the parametrization of the contribution to the total energy,  $E_{xc}$ , due to exchange and correlation effects among the electrons, by a simple term based on the homogeneous electron gas energetics. To facilitate an accurate description of the localized  $f$  electrons of rare earths, the self-interaction correction is introduced. This correction constitutes a negative energy contribution for an  $f$ -electron to localize, which then competes with the band formation energy gained by the  $f$ -electron if allowed to delocalize and hybridize with the available conduction states. The SIC-LSD reduces the overbinding of the LSD approximation for narrow band states. Specifically, the SIC-LSD<sup>29</sup> total energy functional is obtained from the LSD as:

$$E^{SIC} = E^{LSD} - \sum_{\alpha}^{occ.} \delta_{\alpha}^{SIC} + E_{so}, \quad (1)$$

where  $\alpha$  labels the occupied states and  $\delta_{\alpha}^{SIC}$  is the self-interaction correction for state  $\alpha$ . As usual,  $E^{LSD}$  can be decomposed into a kinetic energy,  $T$ , a Hartree energy,  $U$ , the interaction energy with the atomic ions,  $V_{ext}$ , and the exchange and correlation energy,  $E_{xc}$ .<sup>27</sup> The self-interaction is defined as the sum of the Hartree interaction and the exchange-correlation energy for the charge density of state  $\alpha$ :

$$\delta_{\alpha}^{SIC} = U[n_{\alpha}] + E_{xc}[n_{\alpha}]. \quad (2)$$

For itinerant states,  $\delta_{\alpha}^{SIC}$  vanishes identically. For localized (atomic-like) states the self-interaction may be appreciable, and for the free atoms the SIC-LSD approximation was demonstrated to be more accurate than LSD.<sup>29</sup> In Sm compounds, the self-interaction correction term is of the order  $\delta_{\alpha} \sim 80$  mRy per  $f$ -electron. Furthermore, the spin-orbit term is added:

$$E_{so} = \langle \xi(\vec{r}) \vec{l} \cdot \vec{s} \rangle. \quad (3)$$

We employ the atomic spheres approximation, whereby the crystal volume is divided into slightly overlapping atom-centered spheres of a total volume equal to the actual volume. In (3), the angular momentum operator,  $\vec{l} = \vec{r} \times \vec{p}$ , is defined inside each atomic sphere, with  $\vec{r}$  given as the position vector from the sphere center. Other relativistic effects are automatically included by solving the scalar-relativistic radial equation inside spheres.

The  $E^{LSD}$  functional includes the spin-polarization energy, which is a very important contribution in the energetics of SmX compounds. The Sm chalcogenides are non-magnetic,<sup>1</sup> while the pnictides are antiferromagnetic with very low Néel temperatures.<sup>34,35</sup> In the present work the spin-polarized energy functional is not used to describe interatomic magnetism but rather to describe the intra-atomic exchange interactions. By Hund's first rule, the total spin of the  $f^5$  or  $f^6$  ion will be 5/2 or 3, and the ensuing energy gain is reasonably well described with the LSD exchange energy. In this spirit, the delocalization-localization transitions in elemental Ce<sup>36</sup> and Am<sup>37</sup> were described in the LSD approximation as the points of onset of spin polarization of  $f$  bands. In the SmX compounds the effects of a spin-polarized  $f$ -shell have negligible influence on the occupied non- $f$  band states, which are predominantly ligand  $p$  like. An important issue, discussed recently for Eu monochalcogenides,<sup>38</sup> is whether ferro-magnetically ordered Eu  $f^7$  ions can induce a spin splitting of the conduction band states, which can be exploited in spin-filtering.

Of Hund's second and third rules, the latter is governed by the spin-orbit interaction, Eq. (2), which also induces the formation of an orbital moment of the  $f$ -shell. The contribution to the total energy due to the second Hund's rule is, however, not fully accounted for by the spin-orbit interaction alone. The dominating contribution originates from the energy gain by forming the eigenstates of the two-electron interaction  $1/r_{ij}$ , the tetrad effect.<sup>39</sup> Little is known about how to implement these effects in self-consistent solid state calculations. The orbital polarization scheme<sup>40</sup> has had some success in describing the residual orbital moments of itinerant magnets like UFe<sub>2</sub>.<sup>41</sup>

The advantage of the SIC-LSD energy functional in Eq. (1) is that different valency scenarios can be explored by assuming atomic configurations with different total numbers of localized states. In particular, these different scenarios constitute local minima of the same functional,  $E^{SIC}$  in Eq. (1), and hence their total energies may be compared. The state with the lowest energy defines the ground state configuration. Note, that if no localized states are assumed,  $E^{SIC}$  coincides with the conventional LSD functional, i.e., the Kohn-Sham minimum of the  $E^{LSD}$  functional is also a local minimum of  $E^{SIC}$ . The interesting question is, whether competing minima with a finite number of localized states exist. This is usually the case in  $f$ -electron systems<sup>5</sup> and some 3d transition metal compounds,<sup>42</sup> where the respective  $f$  and  $d$  orbitals are sufficiently confined in space to benefit appreciably from

the SIC. The SIC-LSD energy functional in Eq. (1) is a true density functional, as discussed in Ref. 43.

The SIC-LSD still considers the electronic structure of the solid to be built from individual electron states, but offers an alternative description of the single-electron states to the Bloch picture, namely in terms of periodic arrays of localized atom-centered states (*i.e.*, the Heitler-London picture in terms of Wannier orbitals). Nevertheless, there still exist states which will never benefit from the SIC. These states retain their itinerant character of the Bloch form, and move in the effective LSD potential. The resulting many-electron wavefunction will consist of both localized and itinerant states. In contrast to the LSD Kohn-Sham equations, the SIC electron states, minimizing  $E^{SIC}$ , experience different effective potentials. This implies that to minimize  $E^{SIC}$ , it is necessary to explicitly ensure the orthonormality of the one-electron wavefunctions by introducing a Lagrangian multipliers matrix. Furthermore, the total energy is not anymore invariant with respect to a unitary transformation of the one-electron wavefunctions. Both of these aspects make the energy minimization more demanding to accomplish than in the LSD case. The electron wavefunctions are expanded in linear-muffin-tin-orbital (LMTO) basis functions,<sup>44</sup> and the energy minimization problem becomes a non-linear optimization problem in the expansion coefficients. Further details of the present implementation can be found in Ref. 32.

## B. Spectral Functions

Photoemission spectroscopy is a powerful technique for investigations of rare earth compounds.<sup>45</sup> Several studies of the electronic structure of Sm chalcogenides and pnictides by this technique have been reported.<sup>7,15,16,23</sup> The photoemission technique probes the elementary electronic excitations of the material, revealing energy-resolved and - through cross section variations - angular momentum decomposed information. The physical excitation spectrum deviates substantially from the density of states (DOS) of the one-particle states exploited for the minimization of the SIC-LSD total energy. Strictly speaking, the DOS contains information on the one-particle band states that build up the SIC-LSD ground state of the SmX compounds. In view of Janak's theorem,<sup>46</sup> the LSD eigen-energies are good approximations to total energy differences, provided the quasiparticle in question is of extended character. (An unknown shift exists, though, between addition and removal energies.<sup>47</sup>) Therefore, for excitations which are *extended*, like the ideal Bloch waves of band theory, the LSD eigen-energies compare reasonably well with the physical excitation energies. However, often the photon impact creates *localized* excitations. In the SIC-LSD approach one cannot expect the eigen-energies of the localized  $f$ -electrons to have a straightforward physical interpretation. The true many-body character of the elec-

trons in the rare earth compounds is borne out in the multiplet structure of the photoemission spectra, which cannot be reproduced in an independent-particle picture. This shortcoming is also encountered with the LDA and LDA+U approaches. The multiplet structure arises from the two-electron interaction  $U_{ee} = \sum'_{ij} 1/r_{ij}$ , where the prime implies a sum over pairs  $(i, j)$  of electrons. This interaction splits the ionic  $f^n$  configurations into terms characterized by good quantum numbers of orbital, spin and total angular momentum,  $L$ ,  $S$  and  $J$ . In the ground state of the solid usually only the lowest (Hund's rule coupled) term will be populated, maybe others as well if close in energy (within  $k_B T$ , where  $k_B$  is Boltzmann's constant, or a typical  $f$  hybridization energy). But in the final state of the photoemission process, several of the  $f^{n-1}$  terms may be populated and contribute significantly to the spectral features.

Recently, Lichtenstein and Katsnelson<sup>31</sup> devised a simple procedure to augment LDA calculations to describe the multiplet features of partly filled shells. The main ingredient is an atomic selfenergy,  $\Sigma^{atom}(\omega)$ , extracted from the free ion Green's function:

$$G_{\mu\nu}^{atom}(\omega) = \sum_{m,n} g_{mn} \frac{\langle m|c_\mu|n\rangle \langle n|c_\nu^\dagger|m\rangle}{\omega + E_m - E_n + i\delta}. \quad (4)$$

Here,  $m$  and  $n$  enumerate the ion multiplet states with energies  $E_m$  and  $E_n$ ,  $c_\mu$  and  $c_\nu^\dagger$  are, respectively, the annihilation and creation operators of single  $f$ -electrons, and  $g_{mn}$  is a weight factor specifying the relevance of  $m \leftrightarrow n$  transitions. In a thermal environment,

$$g_{mn} = \frac{1}{Z} (e^{-\beta E_m} + e^{-\beta E_n}), \quad (5)$$

where  $\beta = 1/k_B T$  and  $Z = \sum_m e^{-\beta E_m}$  is the partition function. The atomic levels  $|m\rangle$  are found by diagonalization of  $U_{ee}$  in the  $f^n$  manifold:

$$H_{ij}^{atom} = \langle f^n; i | U_{ee} | f^n; j \rangle + n(\epsilon_0 - \mu_F), \quad (6)$$

where  $\epsilon_0$  is the bare  $f$ -level and  $\mu_F$  is the Fermi level. The matrix elements of  $H^{atom}$  are expressed in terms of Slater integrals,  $F^k$ ,  $k = 0, 2, 4, 6$  and Gaunt coefficients,<sup>31</sup> and the Hamiltonian matrix is easily diagonalized numerically. The Slater integrals are calculated using the  $f$  partial waves of the self-consistent LDA calculation.

From the atomic Green's function in Eq. (4) the atomic self-energy is extracted:

$$G^{atom}(\omega) = \frac{1}{\omega - \Sigma^{atom}(\omega)}, \quad (7)$$

and subsequently combined with the LDA Hamiltonian to give the solid state Green's function:

$$G_{\mathbf{k}}^{solid}(\omega) = \frac{1}{\omega - H_{\mathbf{k}}^{LDA} - \Sigma^{atom}(\omega)}. \quad (8)$$

The spectral function is evaluated as the imaginary part of the Green's function of the solid:

$$A^{solid}(\omega) = -\frac{1}{\pi} \text{Im} \sum_{\mathbf{k}} G_{\mathbf{k}}^{solid}(\omega). \quad (9)$$

With care, the spectral function in Eq. (9) may be compared with experimental photoemission spectra. The latter are also strongly influenced by matrix elements as well as secondary electron losses and shake-up effects, all of which are not considered in the present work. When combining the atomic and solid state electronic structure in this fashion, it is important to ensure that no interaction is counted twice. In particular, since the atomic multiplets include the exchange interaction, the band Hamiltonian in Eq. (8) should not be spin-polarized. Also, the LDA Hamiltonian includes the mean Hartree potential, which should therefore also be subtracted in Eq. (6), but this correction is indistinguishable from the Fermi-level adjustment necessary to embed the atom in the solid. This Fermi-level adjustment is the only fitting parameter of the scheme. If more than two  $f^n$  configurations are compared, in practice also a rescaling of the first Slater integral,  $F^0$ , is necessary to achieve results comparable to experimental data. This is due to screening in the photoemission process, which in general renders bare Coulomb interaction too large (by a factor  $\geq 2$ ). A completely analogous screening effect is considered in the LDA+U approach.<sup>6</sup> Lichtenstein and Katsnelson also invoked screening effects of the higher Slater integrals for the interpretation of TmSe photoemission spectra,<sup>31</sup> but this was not considered in the present work. The present approach is similar in spirit to, but differs considerably in details from, the approach of Lehner *et al.* employed for SmS.<sup>4</sup>

### III. RESULTS AND DISCUSSION

#### A. Cohesive Properties

The calculated total energies as functions of unit cell volume are shown in figures 1 and 2, for SmAs and SmS, respectively. In each figure two curves are drawn, corresponding to the two cases of five or six localized  $f$ -electrons on each Sm ion. In SmAs the lowest energy is found for Sm( $f^5$ ) ions, while for SmS the lowest energy is found when assuming localized Sm( $f^6$ ) ions. The energy differences between the  $f^5$  and  $f^6$  minima are  $\Delta E(f^5 - f^6) = -74$  mRy for SmAs and +15 mRy for SmS. The positions of the minima and the curvatures of the  $f^5$  curve for SmAs and the  $f^6$  curve for SmS yield the theoretical equilibrium lattice constants and bulk moduli, which agree well with experimental values, cf. Table I.

To investigate further the electronic structures of the ground states found for SmAs and SmS we show in Fig. 3 the DOS for these two compounds. For both SmAs and SmS, one observes that the ligand  $s$ - and  $p$ -bands are completely filled. In SmAs, two narrow Sm  $f$ -resonances are situated just above the Fermi level. These are the  $f$  majority spin bands for the two  $f$  orbitals which have not been treated as localized. The minority  $f$  bands appear further above the Fermi level. In SmS, similarly, there is

one  $f$  majority orbital which is not localized and therefore appears as a narrow spin-up  $f$  band, in this case  $\sim 3$  eV above the conduction band edge. As a consequence the density of states for SmS reveals a gap of 1.3 eV. This is similar to the gap found in Ref. 3 ( $\sim 2$  eV) and in agreement with the fact that SmS by experimental evidence is a semiconductor. However, the gap in the DOS curve in Fig. 3(b) does not correspond to the physical gap of SmS, which is of  $f \rightarrow d$  character and only  $\sim 0.15$  eV in magnitude.<sup>1</sup> The DOS curves of Fig. 3 do not show the position of the localized states which, as discussed in Section II.B, are not well represented by their respective SIC-LSD eigen-energies. Instead, the localized states can be calculated by total energy differences between the ground state and a state with one  $f$  electron removed. To achieve this a supercell consisting of four SmS formula units was considered, and the total energy calculated for either all Sm atoms in the  $f^6$  configuration, or three Sm atoms in the  $f^6$  configuration and one Sm atom in the  $f^5$  configuration. The missing electron in the latter case is artificially compensated by a uniform positive background, in accord with the scheme often employed for charged impurities in semiconductors.<sup>48</sup> With this approach the lowest  $f \rightarrow d$  transition is found to occur at 0.58 eV below the conduction band edge in the DOS of Fig. 3(b). This is in considerably better agreement with the experimental band gap, albeit still too large, which could be an effect of the limited size of the supercell.

In Fig. 3(c), the density of states of the high pressure ( $f^5$ ) phase of SmS is shown. Compared to the situation in Fig. 3(b) one more electron per formula unit is available for band formation. At the same time, due to the reduced screening of the Sm nuclear charge, the unoccupied  $f$  bands move down in energy. The conduction states are being filled up to the position of the  $f$  resonance, which pins the Fermi level. The inset shows that the first of the two spin-orbit split majority  $f$  bands becomes partly occupied. This means that each Sm ion is in a configuration of mixed  $f^5$  and  $f^6$  character, which we interpret as the SIC-LSD representation of an intermediate valence state, in accord with the conventional wisdom for the golden phase of SmS.<sup>1</sup> The representation of the intermediate valence state, as built from a hybridized band on top of an array of localized  $f^5$  ions, may be a too simplistic description of the true quantum mechanical ground state of intermediate valence, yet due to the variational property of density functional theory it still leads to a good estimate of the binding energy. The lattice constant at the minimum of the SIC-LSD energy curve in Fig. 2, calculated for the high pressure phase,  $a = 5.69$  Å, is in good agreement with the lattice constant obtained for the SmS golden phase,  $a = 5.70$  Å<sup>1</sup> or  $a = 5.65$  Å.<sup>2</sup> We note, however, that the calculated energy balance between the  $f^5$  and  $f^6$  phases in Fig. 2 is at variance with the occurrence of the isostructural transition in SmS already at  $\sim 0.65$  GPa.<sup>14</sup> The common tangent construction applied to figure 2 would lead to a transition pressure of  $\sim 6.5$  GPa, *i. e.* ten times

higher. It is quite conceivable, though, that a more accurate description of the intermediate valence state would lead to higher binding energy for this phase, and hence to a lower transition pressure. With increasing compression in the high pressure  $f^5$  phase the  $f$  band gradually depopulates, at a rate of  $dn_f/d \ln V \sim 0.5$ , in accord with the experimental observation of increasing valency of Sm in the golden phase of SmS with pressure.<sup>9</sup>

From plots similar to those in Figs. 1 and 2 we can deduce the  $f^5$ - $f^6$  energy difference for all SmX compounds. Figure 4 illustrates the trends in this quantity. The calculations reveal a strong preference of the  $f^5$  configuration in the early pnictides, with the energy difference of 135 mRy per formula unit in SmN. For the heavier pnictide ligands, the  $f^6$  configuration becomes more and more advantageous, and for Bi it is only 6 mRy higher than the trivalent configuration. Moving to the chalcogenides, already in the Sm monoxide the  $f^6$  configuration is found to be most favorable, by 6 mRy, and in SmS by 15 mRy. Hence, the SIC-LSD total energy predicts a Sm valency transition between the pnictides and the chalcogenides. This is not in complete agreement with the experimental picture, according to which the divalent and intermediate-valent states are almost degenerate in SmS, while SmO is trivalent and metallic.<sup>49,50</sup> Thus, it appears that the SIC-LSD total energy functional overestimates the tendency to form the divalent configuration of Sm, by approximately 15 mRy, in SmS. Assuming this error is similar for all SmX compounds, this would imply that the calculated energy balance curve in Fig. 4 lies too high by approximately 15 mRy. Therefore, the figure also includes an indication of how the energy difference behaves when a  $\sim 15$  mRy correction is applied (dashed line). This switches the balance in favor of trivalency for SmO, which seems to be in better agreement with experiments, both with respect to the lattice constant and metallicity of SmO.<sup>49,50</sup> In the systematic study of the rare-earth metals and sulphides in Ref. 5 a similar uniform calibration (of 43 mRy) was applied to the trivalent-divalent energy difference of all the rare earths and rare earth sulphides, in order to account for the experimentally observed valencies. The different size of the calibrating energy shift can to a large extent be traced to the neglect of spin-orbit coupling in Ref. 5, and the inclusion of this effect in the present work. In conclusion, the SIC-LSD total energy functional predicts correctly the trends in trivalent-divalent energy difference through the samarium pnictides and chalcogenides, but fails on a quantitative scale of the order of 15 mRy. Such an error is quite reasonable given that the functional does not contain any explicit contribution from the formation of atomic multiplets (the tetrad effect<sup>39</sup>), which would lead to larger energy-lowering for an  $f^5$  ion than for an  $f^6$  ion.

The total energies as a function of volume in the Sm monopnictides and chalcogenides are used to study the basic ground state properties such as equilibrium lattice constant and bulk modulus. The calculated properties are in excellent agreement with the experimental values

which are given in Table I. All lattice constants agree within  $\sim 1\%$  with experiment. Figure 5 compares the calculated lattice constants of the SmX compounds with experimental values and the equilibrium lattice constants of the competing valency configurations.

In view of the intermediate valence interpretation of the high pressure  $f^5$  scenario of SmS depicted in Fig. 3(c), one may wonder if the occurrence of the sharp resonance just above the Fermi level in SmAs in Fig. 3(a) does not also imply a slight admixture of  $f^6$  into the ground state of this compound. Integrating the resonance band, one indeed finds  $\sim 0.11$  occupancy of this band, *i.e.* SmAs is found to have a slightly mixed valent character. The admixture of  $f^6$  character increases to 0.17 in SmSb and 0.30 in SmBi. Neither the experimental photoemission spectra of SmAs nor SmSb show distinct features of  $f^6$  character,<sup>15,23</sup> but on the other hand it is unclear whether a  $\sim 10\%$  admixture of  $f^6$  character could be firmly excluded from the spectra. We are not aware of experiments on SmBi, but the present prediction is that a significant fraction of  $f^6$  should be present in this compound. The proximity of the  $f^6$  states is also probed by doping experiments starting from the pnictide and alloying with chalcogenides.<sup>34,35,53</sup> For SmAs, doping with S or Se does not indicate valence instability for S concentrations up to 40 %<sup>53</sup> or Se concentrations up to 30 %, <sup>34</sup> which suggests that in fact the extra electron of the chalcogen is not transferred into Sm  $f$  states, speaking against the presence of the unoccupied  $f$  band right at the Fermi level. On the other hand, when S is doped into SmSb the valency of Sm is seen to decrease already at low concentrations of S.<sup>35</sup> It seems that more experimental as well as theoretical research, including alloy calculations, is needed to elucidate this issue further.

## B. Valence transitions

As seen in figure 2 the divalent state, with six localized  $f$  electrons on each Sm ion, is the ground state of SmS, however, with compression the intermediate valent phase with five localized  $f$  electrons and some additional band  $f$  electrons becomes more favorable. From a common tangent construction, a transition to the  $f^5$  phase occurs, at a pressure of 0.1 GPa. This is accompanied by a volume reduction of 11.1%. Note, that this transition pressure corresponds to the total energy curves calibrated by the 15 mRy correction discussed in Section III.A.

In the case of SmSe a similar transition is calculated to occur at a pressure of 3.3 GPa with a volume reduction of 9.8%. Experimental evidence shows that SmSe undergoes a continuous transition in the pressure range of 2.6-4 GPa,<sup>54</sup> or 3-8 GPa.<sup>2</sup> The present theory can only describe a discontinuous transition. It has not been resolved whether the continuous volume change is due to the experiments being conducted at room temperature or is an intrinsic property of the quantum state of SmSe. The calculated transition pressure and volume collapse

are in reasonable agreement with the experimental data, cf. Table II, the experimental volume jump being estimated by extrapolation of the divalent  $pV$ -relation over the anomalous region. Note that the two recent experiments quoted above disagree considerably with respect to the pressure range over which the transition occurs.

Similarly to SmSe, experimentally SmTe also exhibits a continuous divalent to intermediate valent transition with pressure. The present theory finds a discontinuous transition occurring at 6.2 GPa with a volume collapse of 8.4%. Again, these values are in good quantitative agreement with the experimental data, cf. Table II.

## C. Photoemission

The spectral functions of SmX compounds are calculated as outlined in Section II.B. Figures 6 and 7 show the spectral functions for SmAs and SmS, respectively. The chemical potential of the reference ion is chosen such that the ground state is  $f^5(^6H)$  for SmAs and  $f^6(^7F)$  for SmS with an energy separation to the lowest  $n-1$  excited levels ( $f^4(^5I)$  of 4.0 eV for SmAs and  $f^5(^6H)$  of 0.8 eV for SmS, respectively), to coincide with the experimental values for these energies. The Slater integrals are almost equal for the two compounds,  $F^k = 23.9, 10.6, 6.5$  and 4.6 eV, respectively, for  $k = 0, 2, 4, 6$  (evaluated with the  $f$ -radial wave at an energy given by the center of gravity of the occupied  $f$ -partial density of states). However, for the direct Coulomb parameter,  $F^0 \equiv U$ , a screened value of  $F^0 = 7.1$  eV was adopted instead of the unscreened value quoted above.

The SmAs spectral function in Fig. 6 shows the four distinct peaks corresponding to the  $f^4(^5L)$ ,  $L = D, G, F, I$ , final states in the photoemission process. These states agree well with the three-peak structure observed by Ref. 23, at binding energies of approximately -10.0 eV, -8.2 eV and -6.0 eV (presuming that the  $^5F$  emission is too weak to lead to a resolvable peak). In the positive frequency region one observes the  $^7F$  peak just above the Fermi level, in accord with the unoccupied majority  $f$ -band in Fig. 3(a). The  $f^6$  final states of  $S = 2$ , which correspond to the unoccupied spin down bands in Fig. 3(a), are situated further up in energy, however now with a considerable spread due to the many allowed multiplets. The position of the corresponding levels in the reference atomic calculation are marked in the figure.

The SmS spectral function is shown in Fig. 7. The spectrum is now characterized by the low binding energy three-peak structure, which is also observed by several experiments,<sup>7,15,23</sup> at binding energies -0.8 eV, -1.5 eV and -4.0 eV, and which is attributed to the  $^6H$ ,  $^6F$  and  $^6P$  final states.<sup>15</sup> The latter state coincides with the S  $p$ -band, as also found in the calculations. The results in Fig. 7 are similar to those obtained by Lehner et al.<sup>4</sup> Recent experiments<sup>7</sup> show traces of Sm  $f^5$  emission in SmS photoemission experiments, possibly also present in older works.<sup>23</sup> It is unclear, whether this is due to small

impurity concentrations or implies a more complicated ground state already for the black phase of SmS. The present total energy calculations have found SmS to be a purely divalent system. It is well known that doping of SmS can lead to the intermediate valence phase, characterized by photoemission spectra of both the high and low binding energy type.<sup>15,23</sup> By carefully tuning the chemical potential of the reference atom in the present theory we can indeed obtain a mixed spectrum, corresponding to a superposition of the spectral functions of Figs. 6 and 7, in good agreement with the spectra recorded for SmAs-SmS alloys.<sup>23</sup> The unoccupied states of SmS have been monitored with bremsstrahlung inverse spectroscopy.<sup>16</sup> The spectra reveal two broad structures, approximately 4.5 and 9 eV above the Fermi level, which are in good agreement with the positions in Fig. 7 of the  $^8S$  and  $^6X$  features, respectively.

#### IV. SUMMARY

The cohesive properties of SmX compounds are well described by the local density approximation to density functional theory provided the self-interaction correction is applied to obtain an improved description of the atomic-like  $f$  electrons. The bonding properties are quantitatively in agreement with experiment as evidenced by accurate lattice constants for both the trivalent pnictides and the divalent chalcogenides. Regarding the energy balance between the trivalent and divalent configurations of Sm in the studied solids (*i.e.* between localized  $f^5$  and  $f^6$  configurations), the SIC-LSD approach seems to underestimate the bonding in the localized  $f^5$  configuration by 10-15 mRy, which can be considered a minor error. However, for an accurate description of the isostructural valence transitions induced by pressure it is a substantial inaccuracy. Correcting for this error we obtain good agreement with high pressure experimental results for SmS, SmSe and SmTe. The high pressure phase of the Sm chalcogenides is described in the SIC-LSD one-electron picture as an array of Sm  $f^5$  ions with an additional partially occupied  $f$ -band, leading to

a total  $f$  occupation between 5 and 6. For SmO, this is found to be the ground state. A small expansion of the SmO lattice, corresponding to an effective negative pressure, would lead to a transition to the divalent and semiconducting phase. This effect could be explored in SmO-SmS alloying experiments.

The occurrence of multiplet effects in the photoemission experiments of SmX compounds is direct evidence that the simple one-electron picture does not suffice to account for all physical characteristics in these compounds. We demonstrated that the inclusion of local atomic correlation effects provides much improved spectral functions, as seen by the close correspondence between the calculated main peaks and experimental photoemission spectra. A certain degree of fitting (of chemical potential and effective Coulomb interaction,  $U$ ) goes into this procedure, which hence cannot be considered as 'ab-initio' as the density functional based total energy calculations. Therefore, substantial further theoretical developments would be needed for a fully parameter free calculation of photoemission spectra.

Concluding, this work has investigated the degree of intermediate valence in Sm pnictides and chalcogenides as manifested in three physical properties, namely the cohesive properties, the pressure characteristics and the photoelectron spectroscopies.

#### V. ACKNOWLEDGEMENTS

This work was partially funded by the EU Research Training Network (contract:HPRN-CT-2002-00295) 'Ab-initio Computation of Electronic Properties of f-electron Materials'. Support from the Danish Center for Scientific Computing is acknowledged. The authors V.K. and G.V. acknowledge the Max-Planck Institute for financial support. The work of L.P. was supported in part by the Defense Advanced Research Project Agency and by the Division of Materials Science and Engineering, US Department of Energy, under Contract No. DE-AC05-00OR22725 with UT-Battelle LLC.

<sup>1</sup> P. Wachter, *Handbook on the Physics and Chemistry of Rare Earths*, Vol. 19, chapter 132 (1994).

<sup>2</sup> T. Le Bihan, S. Darracq, S. Heathman, U. Benedict, K. Mattenberger, O. Vogt, J. Alloys. Comp. **226**, 143 (1995).

<sup>3</sup> R. Schumann, M. Richter, L. Steinbeck, and H. Eschrig, Phys. Rev. B **52**, 8801 (1995).

<sup>4</sup> C. Lehner, M. Richter, and H. Eschrig, Phys. Rev. B **58**, 6807 (1998).

<sup>5</sup> P. Strange, A. Svane, W.M. Temmerman, Z. Szotek, and H. Winter, Nature **399**, 756 (1999).

<sup>6</sup> V. N. Antonov, B. N. Harmon, A. N. Yaresko, Phys. Rev. B **66**, 165208 (2002).

<sup>7</sup> A. Chainani, H. Kumigashira, T. Ito, T. Sato, T. Taka-

hashi, T. Yokoya, T. Higuchi, T. Takeuchi, S. Shin, and N. K. Sato, Phys. Rev. B **65**, 155201 (2002); T. Ito, A. Chainani, H. Kumigashira, T. Takahashi, and N. K. Sato, *ibid.*, 155202 (2002).

<sup>8</sup> S. Raymond, J. P. Rueff, M. D'Astuto, D. Braithwaite, M. Krisch, and J. Flouquet, Phys. Rev. B **66**, 220301 (2002).

<sup>9</sup> A. Barla, J. P. Sanchez, Y. Haga, G. Lapertot, B. P. Doyle, O. Leupold, R. Rüffer, M. M. Abd-Elmeguid, R. Lengsdorf and J. Flouquet, Phys. Rev. Lett. **92**, 66401 (2004); A. Barla, J. P. Sanchez, J. Derr, B. Salce, G. Lapertot, J. Flouquet, B. P. Doyle, O. Leupold, R. Rüffer, M. M. Abd-Elmeguid, and R. Lengsdorf, cond-mat/0406166.

<sup>10</sup> H. Boppart, A. Treindl, and P. Wachter in *Valence Fluc-*

- tuations in Solids* ed. by L. M. Falicov, W. Hanke and M. B. Maple (North-Holland, Amsterdam) p.103 (1981).
- <sup>11</sup> A. Jayaraman, V. Narayanamurthi, E. Bucher, and R. G. Maines, Phys. Rev. Lett. **25**, 1430 (1970).
  - <sup>12</sup> C. M. Varma, Rev. Mod. Phys. **48**, 219 (1976).
  - <sup>13</sup> C. M. Varma and V. Heine, Phys. Rev. B **11**, 4763 (1975).
  - <sup>14</sup> U. Benedict and W. B. Holzapfel, in *Handbook on the Physics and Chemistry of Rare Earths*, Vol. 17, ed. by K. A. Gschneidner, L. Eyring, G. H. Lander, and G. R. Choppin, (North-Holland, Amsterdam 1993) Chapter 113.
  - <sup>15</sup> M. Campagna, E. Bucher, G. K. Wertheim and L. D. Longinotti, Phys. Rev. Lett. **33**, 165 (1974).
  - <sup>16</sup> S.-J. Oh, and J. W. Allen, Phys. Rev. B **29**, 589 (1984).
  - <sup>17</sup> Tu Hailing, G. A. Saunders, and H. Bach, Phys. Rev. B **29**, 1848 (1984).
  - <sup>18</sup> E. Kaldis and P. Wachter, Solid State Commun. **11**, 907 (1972).
  - <sup>19</sup> J. M. D. Coey, S. K. Ghatak, M. Avignon and F. Holtzberg, Phys. Rev. B **14**, 3744 (1976).
  - <sup>20</sup> V. A. Sidorov, N. N. Stepanov, L. G. Khvostantsev, O. B. Tsiok, A. V. Golubkov, V. S. Oskotski, and I. A. Smirnov, Semicond. Sci. Technol. **4**, 286 (1989).
  - <sup>21</sup> A. Jayaraman and R. G. Maines, Phys. Rev. B **19**, 4154 (1979).
  - <sup>22</sup> A. Chatterjee, A. K. Singh, and A. Jayaraman, Phys. Rev. B **6**, 2285 (1972).
  - <sup>23</sup> R. A. Pollak, F. Holtzberg, J. L. Freeouf, and D. E. Eastman, Phys. Rev. Lett. **33**, 820 (1974).
  - <sup>24</sup> O. V. Farberovich, Phys. Stat. Sol. (b) **104**, 365 (1981).
  - <sup>25</sup> P. Strange, J. Phys. C **17**, 4273 (1984).
  - <sup>26</sup> Z. W. Lu, D. J. Singh, and H. Krakauer, Phys. Rev. B **37**, 10045 (1988).
  - <sup>27</sup> P. Hohenberg and W. Kohn, Phys. Rev. **136**, B864 (1964); W. Kohn and L. J. Sham, Phys. Rev. A **140**, 1133 (1965).
  - <sup>28</sup> A. G. Petukhov, I. I. Mazin, L. Chioncel, and A. I. Lichtenstein, Phys. Rev. B **67**, 153106 (2003).
  - <sup>29</sup> J. P. Perdew and A. Zunger, Phys. Rev. B **23**, 5048 (1981).
  - <sup>30</sup> J. Hubbard, Proc. R. Soc. London A **276**, 238 (1963); A **277**, 237 (1964); A **281**, 401 (1964).
  - <sup>31</sup> A. I. Lichtenstein and M. I. Katsnelson, Phys. Rev. B **57**, 6884 (1998).
  - <sup>32</sup> W. M. Temmerman, A. Svane, Z. Szotek and H. Winter, in *Electronic Density Functional Theory: Recent Progress and New Directions*, Eds. J. F. Dobson, G. Vignale and M. P. Das (Plenum, NY 1998.), p. 327.
  - <sup>33</sup> R. O. Jones and O. Gunnarsson, Rev. Mod. Phys. **61**, 689 (1989).
  - <sup>34</sup> R. B. Beeken and J. W. Schweitzer, Phys. Rev. B **23**, 3620 (1981).
  - <sup>35</sup> R. B. Beeken, W. R. Savage, J. W. Schweitzer, and E. D. Cater, Phys. Rev. B **17**, 1334 (1978).
  - <sup>36</sup> D. Glötzel, J. Phys. F **8**, L163 (1978).
  - <sup>37</sup> H. L. Skriver, O. K. Andersen and B. Johansson, Phys. Rev. Lett. **44**, 1230 (1980).
  - <sup>38</sup> M. Horne, P. Strange, W. M. Temmerman, Z. Szotek, A. Svane and H. Winter, J. Phys. Condens. Matter (to appear, 2004)
  - <sup>39</sup> C. K. Jørgensen, *Orbitals in Atoms and Molecules* (Academic, London, 1962); L. J. Nugent, J. Inorg. Nucl. Chem. **32**, 3485 (1970).
  - <sup>40</sup> M. S. S. Brooks, Physica **130 B-C**, 6 (1985); O. Eriksson, M. S. S. Brooks and B. Johansson, Phys. Rev. B **41**, 7311 (1990).
  - <sup>41</sup> M. S. S. Brooks, T. Gasche, O. Eriksson, L. Severin and B. Johansson, J. Alloys. Comp. **213/214**, 238 (1994).
  - <sup>42</sup> A. Svane and O. Gunnarsson, Phys. Rev. Lett. **65**, 1148 (1990); Z. Szotek, W. M. Temmerman and H. Winter, Phys. Rev. B **47**, 4029 (1993).
  - <sup>43</sup> A. Svane, Phys. Rev. B **51**, 7924 (1995).
  - <sup>44</sup> O. K. Andersen, Phys. Rev. B **12**, 3060 (1975); O. K. Andersen and O. Jepsen, Phys. Rev. Lett. **53**, 2571 (1984).
  - <sup>45</sup> M. Campagna, G. K. Wertheim and Y. Baer, in *Photoemission in Solids II*, Eds. L. Ley and M. Cardona, (Springer, Berlin, 1979), ch. 4.
  - <sup>46</sup> J. F. Janak, Phys. Rev. B **18**, 7165 (1978).
  - <sup>47</sup> J. P. Perdew and M. Levy, Phys. Rev. Lett. **51**, 1884 (1983); L. J. Sham and M. Schlüter, Phys. Rev. Lett. **51**, 1888 (1983).
  - <sup>48</sup> U. Gerstmann, P. Deak, R. Rurali, B. Aradi, Th. Frauenheim, and H. Overhof, Physica B **340**, 190 (2003). No explicit correction term was employed in the present study.
  - <sup>49</sup> J. M. Leger, P. Aimonino, J. Loriers, P. Dordor, and B. Coqblin, Phys. Lett. **80A**, 325 (1980).
  - <sup>50</sup> G. Krill, M. F. Ravet, J. P. Kappler, L. Abadli, J. M. Leger, N. Yacoubi, and C. Loriers, Solid State Commun. **33**, 351 (1980).
  - <sup>51</sup> P. Villars and L. D. Calvert, *Pearson's Handbook of Crystallographic Data for Intermetallic Phases*, 2. ed., (ASM International, Ohio, 1991).
  - <sup>52</sup> I. Shirovani, K. Yamanashi, J. Hayashi, Y. Tanaka, N. Ishimatsu, O. Shimomura, T. Kikegawa, J. Phys. C **13**, 1939 (2001).
  - <sup>53</sup> S. Von Molnar, T. Penny, F. Holtzberg, J. De. Phys. C **4**, 241 (1976).
  - <sup>54</sup> O. B. Tsiok, V. A. Sidorov, V. V. Bredikhin, L. G. Khvostantsev, A. V. Golubkov, and I. A. Smirnov, Solid State Commun. **79**, 227 (1991).



Compound	Lattice constant (a.u)		Bulk modulus (GPa)	
	Present	Expt. <sup>a</sup>	Present	Expt.
SmN	9.46	9.52	131	-
SmP	10.99	10.88	68.7	-
SmAs	11.18	11.16 <sup>f</sup>	67.6	84.2(3.5) <sup>b</sup> , 78.3 <sup>i</sup>
SmSb	11.90	11.84	46.7	-
SmBi	12.14	12.01	41.3	-
SmO	9.41	9.34 <sup>g</sup>	106.6	-
SmS	11.25	11.25 <sup>f</sup>	53.4	42(3) <sup>c</sup> , 50.3 <sup>d</sup> , 47.6(5.0) <sup>e</sup>
SmSe	11.70	11.66	53.4	40(5) <sup>c</sup>
SmTe	12.43	12.46	37.6	40(5) <sup>c</sup>
SmPo	12.64	12.71 <sup>h</sup>	33.4	-

TABLE I: Calculated lattice constant and bulk moduli of SmX compounds in the NaCl structure. The Sm ions are in the calculated ground state configuration of  $f^5$  for the pnictides and SmO, and of  $f^6$  for the other chalcogenides.

<sup>a</sup>: Reference 51, except where reference to other work is given.

<sup>b</sup>: Reference 52.

<sup>c</sup>: Reference 14.

<sup>d</sup>: Reference 17.

<sup>e</sup>: Reference 18.

<sup>f</sup>: Reference 23 at 110 K.

<sup>g</sup>: Reference 50.

<sup>h</sup>: Sm<sub>0.532</sub>Po<sub>0.468</sub>.

<sup>i</sup>: Reference 53.

Compound	$P_t$ (GPa)		Volume collapse (%)	
	Theory	Expt.	Theory	Expt.
SmS	0.1	0.65 <sup>a</sup> , 1.24 <sup>c</sup>	11.1	13.5 <sup>a</sup> , 13.8 <sup>c</sup>
SmSe	3.3	$\sim 4^a$ , 3.4 <sup>b</sup> , 3 – 9 <sup>c</sup> , 2.6 – 4 <sup>d</sup>	9.8	8 <sup>a</sup> , 11 <sup>c</sup> , 7 <sup>d</sup>
SmTe	6.2	2 – 8 <sup>a</sup> , 5.2 <sup>b</sup> , 6 – 8 <sup>c</sup> , 4.6 – 7.5 <sup>d</sup>	8.4	9 <sup>c</sup> , 7 <sup>d</sup>

TABLE II: Calculated isostructural transition pressures,  $P_t$  (in GPa), and volume changes (in %), of Sm monochalcogenides. Experimentally, the transitions of SmSe and SmTe (at room temperature) are continuous, while SmS exhibits a discontinuous volume change. The calculated transition pressures include the 15 mRy calibration of the total energy calculated for the high pressure phase (see text).

<sup>a</sup>: Reference 14.

<sup>b</sup>: Insulator-metal transition of Reference 20.

<sup>c</sup>: Present author's estimates from figures of Reference 2 and <sup>d</sup>: Reference 54. The volume changes for SmSe and SmTe are obtained by extrapolation over the transition range.

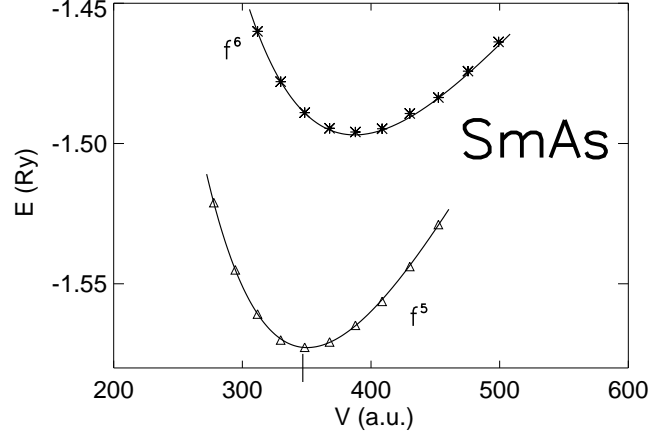


FIG. 1: SIC-LSD total energy versus unit cell volume for SmAs. The two curves correspond to trivalent and divalent Sm ions, realized by localized  $f^5$  (triangles) and  $f^6$  (stars) configurations, respectively. The vertical bar on the  $V$ -axis marks the experimental equilibrium volume.

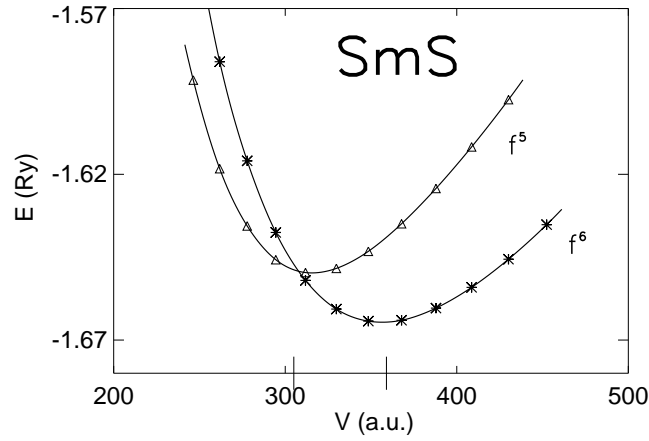


FIG. 2: SIC-LSD total energy versus unit cell volume for SmS. The two curves correspond to trivalent and divalent Sm ions, realized by localized  $f^5$  (triangles) and  $f^6$  (stars) configurations, respectively. The data presented do not include the 15 mRy calibration for the  $f^5 - f^6$  energy difference (see text for discussion). The vertical bars on the  $V$ -axis marks the experimental volumes of the black and golden phases.

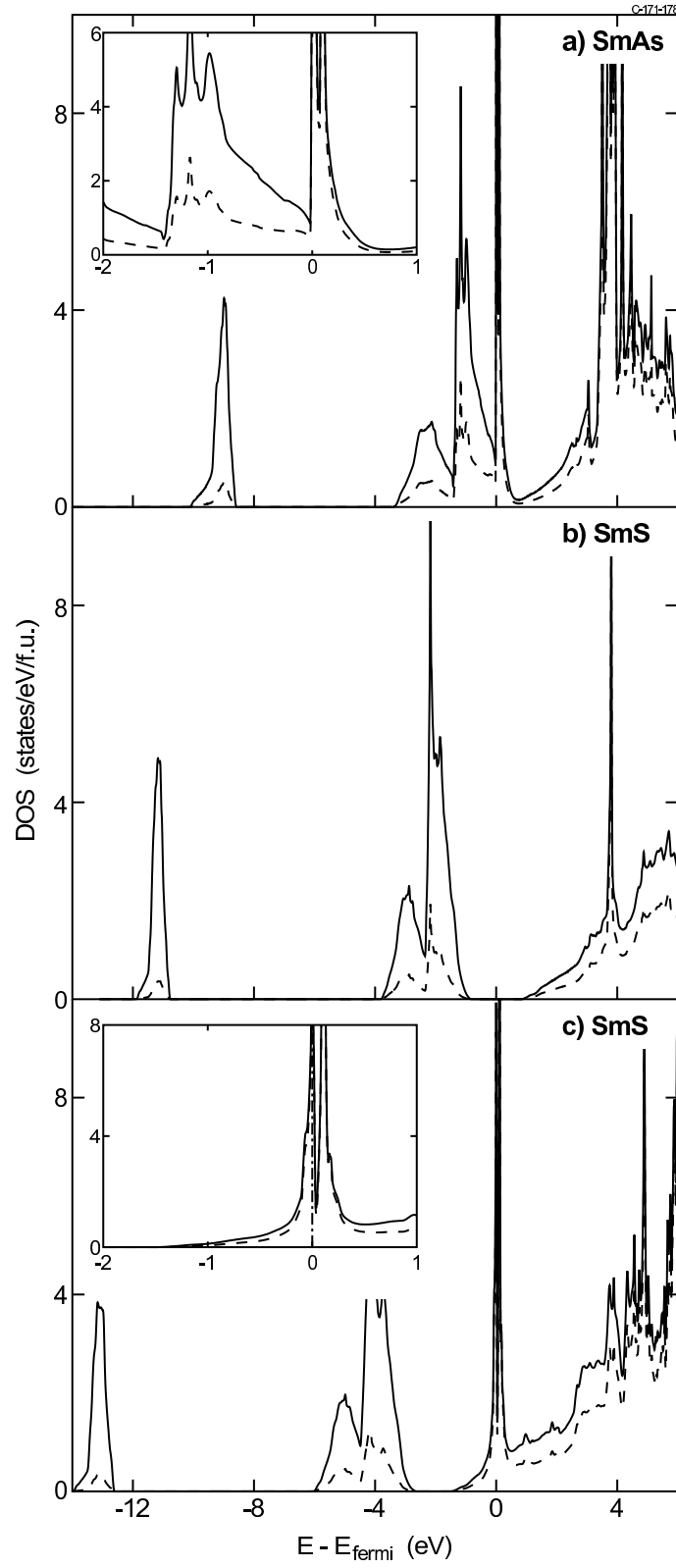


FIG. 3: SIC-LSD densities of states (DOS) for: a) SmAs with localized  $f^5$  Sm ions ( $a = 11.18$  a.u.), b) SmS with localized  $f^6$  Sm ions ( $a = 11.25$  a.u.), and c) high pressure phase of SmS with localized  $f^5$  Sm ions ( $a = 10.75$  a.u.). Energies are given relative to the Fermi level. The units of the DOS is states per eV and per formula unit. The full line is the total DOS, while the dashed line shows the DOS projected onto the Sm atom. The insets in a) and c) show a blowup of the region in the vicinity of the Fermi level.

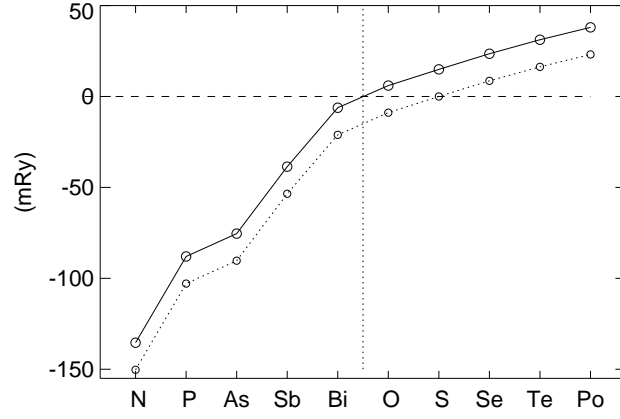


FIG. 4: Trivalent-divalent energy difference (in mRy per formula unit) of Sm compounds (full line). A negative sign implies that the trivalent state is favored. The dashed line marks the corrected energy curve (see text).

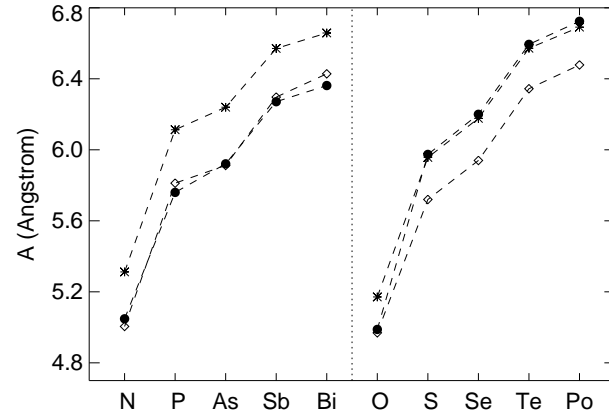


FIG. 5: Comparison of experimental and theoretical lattice constants (in Ångström) of SmX compounds. Experimental values (see Table I) are marked with solid circles, while lattice constants calculated assuming a divalent (trivalent) Sm configuration are marked with stars (diamonds).

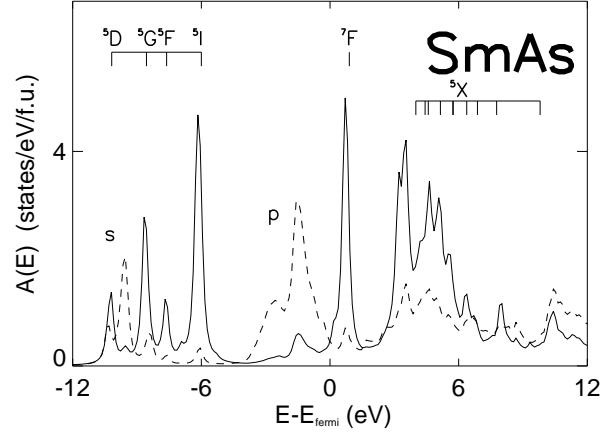


FIG. 6: The calculated spectral function of SmAs at equilibrium volume,  $a = 5.91$  Å. The full curve shows the  $f$ -contribution and the dashed curve the non- $f$  contribution. The energy is given relative to the Fermi level. The main lines are characterized by their final state characteristics, either As  $s$ ,  $p$ -bands, or  $f^{n\pm 1}$  multiplet term.

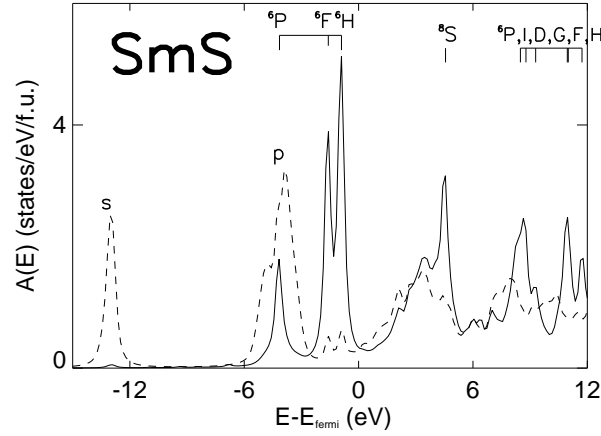


FIG. 7: The calculated spectral function of SmS (black phase,  $a = 5.95$  Å). The full curve shows the  $f$ -contribution and the dashed curve the non- $f$  contribution. The energy is given relative to the Fermi level. The main lines are characterized by their final state characteristics, either S  $s$ ,  $p$ -bands, or  $f^{n\pm 1}$  multiplet term.